Inter-building assessment of urban heat island mitigation strategies: field tests and numerical modelling in a simplified-geometry experimental set-up

Abstract

Large scale mitigation strategies showed to represent promising solutions for enhancing liveability in dense urban contexts. Therefore, most of the researches are focused on assessing the effect of high albedo surfaces and greenery. The paper deals with a numerical and experimental analysis of these evapotranspiration and high-reflectance surfaces in a full scale experimental set-up where more than 20 cubicles are monitored in a Mediterranean continental climate. The experimental set-up itself covers an intermediate inter-building perspective between the lab scale and the real urban contexts, which compromises the possibility to generalize final results. This scale is able to better control geometry of area, but allows real microclimate monitoring and calibration of CFD models. Starting from a validated model, this study simulated alternative scenarios with gradually varying the presence of common mitigation strategies with the scope to evaluate their effect to this aim. Results showed that high albedo solutions best mitigate summer overheating reducing the air temperature, while greenery was more effective in the densest configurations with low albedo envelopes, showing how geometry related variables may play a key role in determining the optima configurations of microclimate mitigation strategies, also important for the best exploitation of renewables in the built environment.

Keywords: Urban heat island; microclimate mitigation; green roof and façade; cool pavement; energy efficiency; inter-building effect.

1. Introduction

The increase of the building energy demand to about 40% of the total energy demand in developed countries and the expected concentration of more than 65% of the population within urban environments by 2050 worldwide highlighted the severe need to improve building energy efficiency and, on top of that, new microclimate conditions characterized by anthropogenic local scale climate change related to this acknowledged phenomenon [1][2][3]. Therefore, a variety of studies were written in the last decades about energy efficiency in buildings and urban heat island (UHI) mitigation techniques, demonstrating how a consistent greenery design and the implementation of cool

pavements and building envelope may hugely contribute to counteract UHI effect in dense city developments [4][5][5] and save energy if applied as passive cooling solutions. For example, more than 200 cities were monitored and UHI is indeed the most acknowledged climate change related phenomenon, and has a big responsibility in exacerbating heat waves and health risks consequent to that short time events which lately rapidly increased their happening frequency [6][7][8]. Many of these studies focused on the single-building scale implementation of greenery-based solutions and cool materials, demonstrating how cool and green roofs, for instance, may drastically reduce building energy demand in cooling seasons around the world [10,11] or they focused on the analysis of building energy demand with considering UHI-generated local boundary conditions [9]. In detail, Rosso et al. [10] demonstrated how cool and green pavements are able to improve people wellbeing perception and outdoor comfort. Additionally, if applied over roofs as energy efficiency strategy, cool materials may be responsible for almost 40% of energy savings with almost negligible penalties in winter in the case of high albedo roofs, mostly due to the relatively weaker solar radiation in winter and the more frequent turbulent convection generated by large thermal differences in heating conditions in residential buildings [12,13]. Of course their effectiveness is also very much depending on other actions such as occupancy and, more in general, awareness of occupants about passive cooling strategies, that should be considered while quantitatively assessing their performance in the indoors [11].

Another important group of studies is focused on microclimate analysis through field monitoring and CFD simulation, where mitigation solutions are assessed and their impact on outdoor thermal comfort is investigated [14,15]. In detail, Efthymiou et al. [12] investigated the effect of PV-integrated pavements for mitigating UHI by means of numerical techniques validated with outdoor monitored data, confirming their surface temperature abatement by about 5 K. The same analysis, together with specific thermal comfort assessment in the outdoors, is also carried out in historical contexts, such as in Rome, where it is typically more difficult to implement such mitigation strategies due to architectural constraints, as described by Laureti et al. [13].

Therefore, building materials and mitigation techniques are fundamental in order to allow wellbeing and operations in both the indoors and outdoors in those climate areas where also external activities are frequently carried out by several cultures, such as in the Mediterranean areas [14][15][16] and in other mild and tropical climates [17][18][19].

Most of such microclimate CFD-based studies are implemented in real urban contexts where field data may be collected but also where the results are pretty case specific, since most of the mitigation strategies do not present fully replicable methods and findings. At the same time, parametric studies

are not representing realistically enough the urban contexts, since most of them concern simple and regular geometries, which are absolutely not representative of realistic urban systems, in developed countries in particular, where the architectural multilayer structure was designed and constructed over the centuries [20][21]. In fact, microclimate assessment and mitigation showed to be very much affected by specific geometry issues, as demonstrated by E. Ng et al. [22]. They studied the cooling effect of green roofs in a high-rise and high-density city, and concluded that neither planting vegetation nor planting grass is effective in cooling the pedestrian environment. Also they affirmed that when the building-height-to-street-width ratio exceeds 1, the benefit of cooling effect grade is low. Therefore, the cooling benefits are realistically effective when building heights are low (20 m) compared to tall (at 40 m or 60 m). On the contrary, they concluded that "the cooling effect of about 1 K is possible when tree coverage is larger than 1/3 of the total area".

Therefore, this study wants to contribute to the scientific knowledge of UHI mitigation techniques at inter-building scale by providing an exhaustive investigation in between parametric simplified built environment and real scale in-situ experiments, very much affected by case specific conditions and local peculiarities. In order to bridge this gap, the analysis at inter-building scale is carried out by means of calibrated microclimate simulation of a real construction field populated by prototyped buildings (i.e. cubicles with representative dimensions). The simple geometry of such a field allowed to easily control microclimate variations due to changes on single variable like pavement optical properties or greenery implementation. Therefore, the obtained simulations' outputs give the chance to perform pretty general observations and conclusions on the effectiveness of specific interventions on the outdoor but, at the same time, to refer to a real field constantly monitored in terms of microclimate conditions. Moreover, field-collected weather data are used to trigger and then calibrate the microclimate model. The model itself is then analysed with designing and implementing classic microclimate mitigation strategies at inter-building level, represented by green envelope and pavements' cool materials, and varying distances among the modelled buildings to assess the efficacy of the proposed strategies in different configurations. The main results are then able to quantify the effect of such solutions in the climate conditions of Lleida, a Spanish city close to Barcelona, and to be representative for driving potential large scale and effective urban design strategies in that area.

2. Methodology

2.0 Framework of the research

The modelled area is the experimental set-up located at Puigverd de Lleida (Spain) [4] where several active and passive building energy saving strategies are tested [23]. Among the tested strategies there

are also green systems, such as green facades [24][25]and green roofs, which are the reference green systems adopted for the simulation. The adopted procedure can be summarized in the following steps:

- Microclimate modelling of the Puigverd de Lleida experimental set-up and model calibration by means of weather data directly collected in the area.
- Simplification of the modelled area in order to get three different and comparable scenarios, i.e. basic (no greenery), 100% green roof, and 100% southern green facade scenario.
- Evaluation of the microclimate mitigation potential of green systems when combined with different outdoor pavement characteristics, i.e. natural soil and artificial covering presenting low, medium and high level of albedo.
- Evaluation of the microclimate mitigation potential of the above mentioned strategies, i.e. green systems and cool pavements, varying the cubicle mutual-distances and therefore the geometrical characteristics of the investigated settlement.

All the above-mentioned steps are presented in details in the following sections of the work.

2.1. Description of the case study: Puigverd de Lleida experimental set-up

The real-scale pilot plant modelled in this study is located at Puigverd de Lleida, in the Northeast area of Spain under a Mediterranean Continental Climate. In particular, the area is classified as Csa climate accordingly to the Köppen-Geiger classification: semi-arid climate with mild and foggy winters and dry and hot summers [26]. More specifically, the summers are hot and mostly clear, the winters are cold and partly cloudy, and it is dry year round. Over the course of the year, the temperature typically varies from 0°C to 35°C. The hot season lasts for 3.0 months, from June 11th to September 10th, with an average daily high temperature above 29°C. For that reason, the study took place in that period of the year.

Puigverd de Lleida is a mainly agricultural context and the urban centre closest to the set-up is at 450 m as the crow flies. The experimental set-up is planned in order to test both active and passive solutions for energy efficiency in prototype buildings through the application of different materials, technologies and building construction systems on very simplified house-like cubicles. The facility consists of 22 cubicles shown in Figure 2, 16 different single cubicles with same inner dimensions (2.4 m × 2.4 m × 2.4 m), 3 double-height cubicles (2.4 m× 2.4 m× 5.1 m) and 3 double width-cubicles (2.4 m× 5.25 m × 2.4 m). [23]. Such cubicles are North-South oriented, and their mutual distance (9 m) is designed to avoid mutual-shading. The whole experimental set-up is continuously monitored to analyse the thermal performance of each tested technology. Weather data are collected every five minutes in proximity of the southern border of the experimental field. The recorded meteorological

parameters consist of solar global radiation [W/m^2], wind speed [m/s], wind direction [°], external air temperature [°C], and relative humidity [%]. More in detail, the weather station includes two MIDDLETON SOLAR meters SK08 to capture horizontal and vertical global solar radiation, an ELEKTRONIK EE21 probe with a metallic shield to be protected against radiation to measure the outer air and humidity, and finally a DNA 024 anemometer for the wind speed and direction. At the same time, all cubicles built to test passive systems are equipped with six internal wall temperatures, an indoor thermo-hygrometer, and two heat flux meters applied on the southern wall. In addition, four extra temperature probes are implemented in correspondence of the tested green vertical systems to measure temperatures on the external wall surfaces, the air gap between the wall and the green curtain, the green systems, and 5 cm beyond the green wall, i.e. 50 cm far from the building wall surface [24].

2.2. Microclimate modelling and calibration

The numerical simulation of the Puigverd de Lleida experimental set-up was done through the 3D validated microclimate modelling system ENVI-met V4 [27]. The adopted tool demonstrated to be particularly suitable for the final purpose of the study since it guarantees good resolution in space allowed by the use of the orthogonal Arakawa C-grid numerical discretization scheme [28]. The wind field is derived by the Reynolds-averaged non-hydrostatic Navier-Stokes equations (RANS) which are solved at each point of the 3D grid and for each chosen time step, i.e. one second. Additionally, turbulence is considered by the application of the Turbulence Kinetic Energy (TKE) model which describes kinetic energy distribution and its dissipation rate. Therefore, the software calculates the outdoor air temperature and relative humidity taking into account both short- and long-waves radiation fluxes considering all the thermo-physical properties of the building components, i.e. thickness, solar reflectance, thermal emissivity, absorption capability, transmission capability, heat transfer coefficient, and heat capacity. The surface temperature and the distribution of soil temperature is evaluated for both natural and artificial materials down to 4 m below the surface.

The model presents a mesh unit dimension of 1x1x1 m for a total model extension of 64x80x35 m. The grid size allows to reduce at minimum the geometrical simplification of the tested experimental field which is already characterized by a strict simplified geometry. The envelope of each cubicle of the camp is modelled by taking into account the real stratigraphy of the reference cubicle and therefore its characteristics already experimentally detected [23]. Moreover, the adopted terrain profile is directly derived from the site-specific EnergyPlus database [29] i.e. prevalent clay terrain, and the settled soil albedo experimentally derived by means of an albedometer. In details, the adopted

device consists in two pyranometers combined into one instrument and characterized by the same technical specifications given in Table 1.

Table 1. Albedometer technical details

Spectrum range	305-2800 nm
Irradiance range	0-2000 W/m^2
Sensitivity	10-15 μV/(W/m^2)
Response time	16 s

The terrain albedo measurement campaign is carried out by positioning the instrument alternatively upon a bare and a grassy portion of the terrain during a sunny day, i.e. from 12:00 pm to 2:00 pm. The measurements last both one hour with a recoding interval of 2 minutes. The saturated terrain albedo was therefore settled at 0.14 since from the experimental data no significant differences were outlined between the bare and grassy terrain portions, i.e. average albedo value of 0.14 and 0.15 respectively.

The meteorological station data recorded during a sunny summer day, i.e. June 21st, are used as input for the microclimate simulation (Table 2). The air temperature and relative humidity hourly profiles of the selected day are presented with respect to the seasonal average profiles in Figure 1. The day chosen for the simulation is representative of summer conditions in the area especially during the hottest hours of the day which are the most threatening for human health, i.e. from 12 p.m. to 8 p.m.

Table 2. Weather input parameters derived from experimentally collected data

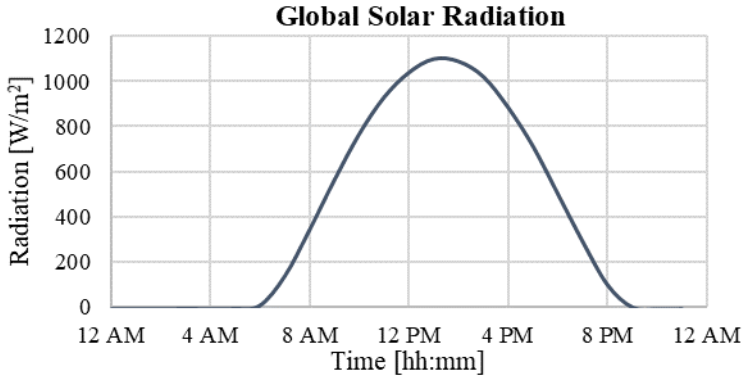

Wind speed (10 m)	1.5 m/s
Wind direction	173.9°

time am	**12**	**01**	**02**	**03**	**04**	**05**	**06**	**07**	**08**	**09**	**10**	**11**
Air temperature [°C]	18.9	18.1	15.4	14.8	13.9	12.8	12.6	16.5	22.5	23.3	25.1	26.8
Relative humidity [%]	72.6	76.2	88.0	90.1	95.1	95.1	96.4	86.7	63.2	56.7	50.6	45.6

time pm	12	01	02	03	04	05	06	07	08	09	10	11
Air temperature [°C]	29.5	30.1	31.5	32.5	33.3	34.0	33.5	32.3	29.6	25.7	22.2	20.9
Relative humidity [%]	38.3	36.6	33.5	31.1	27.7	24.5	31.2	35.5	45.1	56.3	69.2	75.1

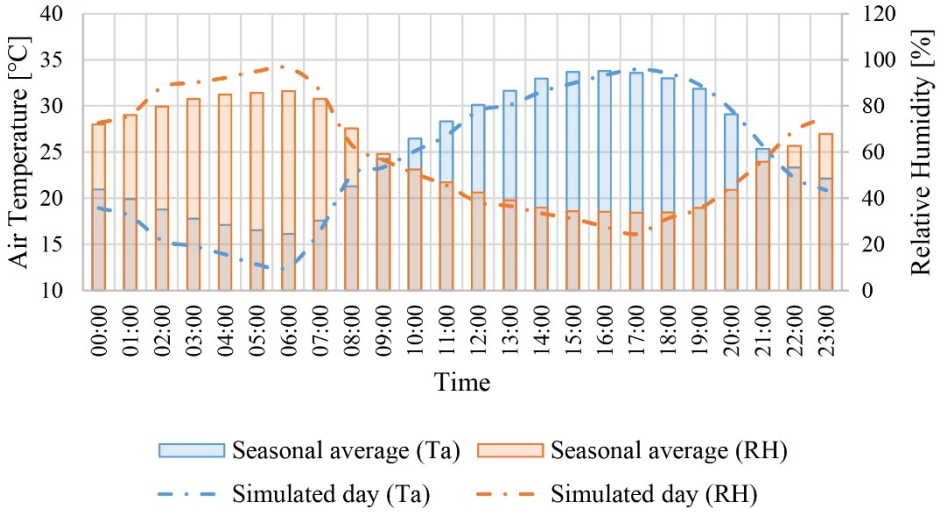

Figure 1. Hourly air temperature and relative humidity profiles of both (i) the simulated day and (ii) the average day for the summer season.

The calibration is therefore performed comparing data collected within the set-up by the available external air temperature probes and the simulation output of air temperature extracted in correspondence of the real sensors position, 0.5 m far from the cubicle surfaces and at 1.5 m height from the ground (Figure 2a, points 1 and 2) [24][23]. Moreover, the simulated data close the model southern board are compared to the collected weather data in terms of air temperature and relative humidity (Figure 2a, point 3).

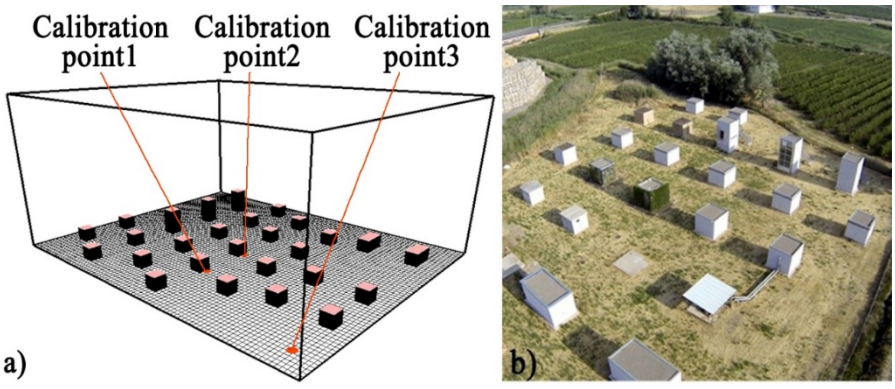

Figure 2. (a) Calibration points within the Puigverd de Lleida microclimate model and (b) aerial view of the experimental set-up.

Finally, the model accuracy is verified through the calculation of the most common used validation indexes [30] which are the following:

- Mean Bias Error (MBE), describing the bias between simulated (S) and observed (O) values (Eq. 1):

$$MBE = N^{-1} \sum_{i=1}^{N} (S_i - O_i) \quad \text{(Eq. 1)}$$

- Systematic Root Mean Square Error ($RMSE_S$), the RMSE due to reliability of the model which should approach zero (Eq. 2):

$$RMSE_s = \sqrt{N^{-1} \sum_{i=1}^{N} (\widehat{S_i} - O_i)^2} \quad \text{(Eq. 2)}$$

where $\widehat{S_i}$ is the simulated variable according to the least-squares regression, $\widehat{S_i} = a + b \cdot O_i$

- Unsystematic Root Mean Square Error ($RMSE_U$), the RMSE complementary part to $RMSE_S$:

$$RMSE_U = RMSE - RMSE_S \quad \text{(Eq. 3)}$$

- Willmot index of agreement (d), descriptive measure varying between 0 and 1:

$$d = 1 - \left[\sum_{i=1}^{N} (S_i - O_i)^2 / \sum_{i=1}^{N} (|S'_i| + |O'_i|)^2 \right] \quad \text{(Eq. 4)}$$

where $S'_i = S_i - \bar{O}$ and $O'_i = O_i - \bar{O}$

2.3. Generation of the mitigation scenarios

Considering the calibrated model as reference scenario, 36 different models are generated to assess UHI mitigation potential of both (i) green systems and (ii) external pavements' albedo within contexts with different (iii) building density. More in details, three different models are then generated taking into account the application of green systems:

- the basic scenario (B_) presenting all the cubicles characterized by the same envelope and the total absence of applied greenery systems;
- the 100% green roof scenario (Gr_) where a layer of greenery is applied upon the roofs of all the camp cubicles;
- the 100% southern green facades scenario (Gf_) where a specifically designed vertical green element was applied on the southern facade of each cubicle in the model.

More in detail, the greenery systems adopted for the two mitigation scenarios, i.e. Gr and Gf, were realized considering the experimental characterization of the green systems actually developed and tested in Puigverd de Lleida [23]. In particular, the settled albedo, i.e. 0.14, was experimentally detected by means of the albedometer following the same procedure described above for the terrain albedo evaluation, i.e. instrument positioned alternatively on different portions of the green system during a sunny day between 12:00 pm and 2:00 pm (Figure 3).

Figure 3. Albedo monitoring (a) of the green roof tested in Puigverd and (b) of the natural ground in the experimental field; (c) Green wall façade; (d) Green Roof.

Moreover, the LAD profile, i.e. Leaf Area Density profile, was settled equal to 0.3 m^2/m^3 for both the vertical and the horizontal system considering such value representative of the existing green roof and of the green extensive wall installed. Nevertheless, further research focusing on LAD is needed since previous studies considered different LAD values for similar green systems [31] and still today it is a controversial index that can affect significantly the results.

In addition, all the presented scenarios are simulated with varying the superficial properties of the terrain for a total amount of four different models for each above described scenario, i.e. total amount of 12 combinations. In particular, the upper layers of natural soil, i.e. clay terrain, adopted for the reference scenario are replaced by an artificial material, i.e. mineral concrete, in order to depict an environment much closer to a real urban area and to test the effectiveness of cool pavements against the UHI phenomenon even coupled with the modelled greenery systems. In fact, the artificial material is applied with three different values of albedo (a) derived from literature [16]:

- low albedo scenario, (_La) albedo equal to 0.14, which is the same albedo of the natural reference soil completely wet;
- medium albedo scenario, (_Ma) albedo equal to 0.30;
- high albedo scenario, (_Ha) albedo equal to 0.65;

Table 3. Summary of the performed simulations and referring acronyms

	Greenery:	Basic Scenario (B)	Green Roofs (Gr)	Green Facades (Gf)
Outdoor pavements:				
Natural ground, Puigverd (Gp)		BGp	GrGp	GfGp
Artificial High Albedo (Ha)		BHa	GrHa	GfHa
Artificial, Medium albedo (Ma)		BMa	GrMa	GfMa
Artificial, Low albedo (La)		BLa	GrLa	GfLa

All the presented scenarios are tested with the following Aspect Ratio (AR):
AR(3/9)=0.33, AR(3/5)=0.6, AR(3/3)=1

Finally, the geometrical configuration of the area is modified always in order to make the modelled experimental test-field much closer to a simplified urban environment. Moreover, changes of the model geometry allow to test how the urban configuration in terms of aspect ratio, i.e. height-width ratio of urban canyons, affect the effectiveness of the modelled strategies, i.e. application of greenery systems and cool pavements. The house-like cubicles mutual distance is progressively reduced from 9 m, i.e. real configuration, down to 3 m. In particular, this study presents a comparative analysis of the modelled configurations with a cubicles mutual distance of 9 m, 5 m, and 3 m. A summary of the whole above mentioned elaborated models is given in Table 3.

All the presented scenarios are simulated under the same input weather forcing adopted for the model validation which is representative of a sunny summer day in Lleida (Spain). Each simulation lasted 48 hours, to provide 24 hours of training stage to the model [32]. The results presented and discussed in the following section are given by the last 24 hours simulated. In particular, results are presented in terms of (i) daily profile and (ii) spatial distribution of the environmental parameters of interest. The presented daily profiles are derived averaging the air values extracted at 1.5 m from the ground (human torso height for a standard man) in four selected points representative of the canyons surrounding the inner reference cubicle (Figure 5b). This procedure allows to get environmental

conditions within the modelled area without specific affection due to canyons orientation. The spatial distribution within the modelled area is given by sections made at both 1.5 m and 3.5 m from the ground at selected times of the day, i.e. 6 am, 11 am, 4 pm, and 12 am. In particular, the chosen sections' heights allow to get data spatial distribution at pedestrian level and just above the cubicles' rooftop. The chosen times give an overview of the environmental parameters daily trend with specific reference to their values at the end of the night, i.e. 6 am, just before the sun radiation peak, i.e. 11 am, at air temperature peak, i.e. 4 pm, and 5 hours after the sunset, i.e. 12 am.

3. Results and discussion

3.1. Microclimate model validation

The 24 hours temperature profiles of both simulated and observed data are compared as reported in Figure 4. A good correspondence among simulated and observed values is evident at the calibration points 1 and 3 while at point 2 discrepancies are detected during the hottest hours of the simulated day, i.e. from 12:00 pm to 5:00 pm. Nevertheless, the detected rapid temperature increase suggests that the observed values are may affected by direct solar radiation hitting the probe while is quite realistic the simulated air temperature profile. The calculated validation indexes are reported in Table 4. The presented values allow to consider the model validated according to the literature references [33].

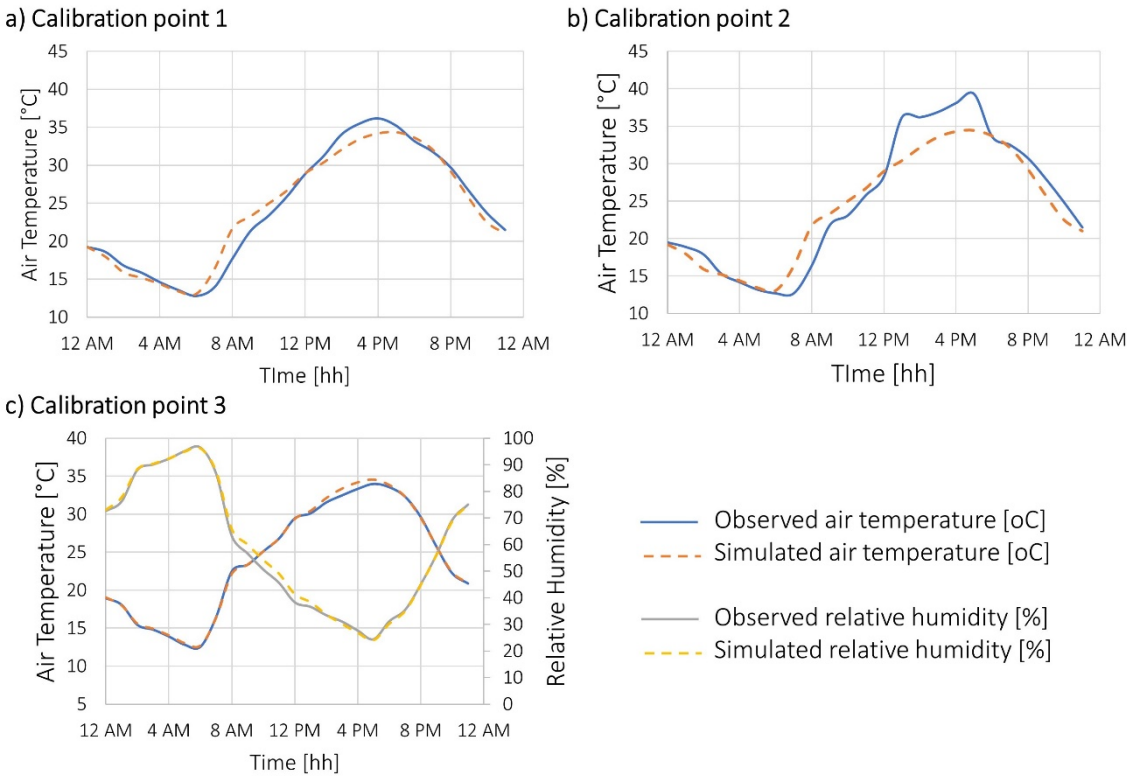

318

319 **Figure 4.** Comparison of the observed and simulated temperature profiles at the three selected
320 calibration points.

321

322 **Table 4. Validation indexes calculated at the three selected calibration points**

Calibration point	MBE [°C]	RMSEs [°C]	RMSEu [°C]	d
Point 1	-0.05	0.93	2.07	0.99
Point 2	-0.71	1.87	3.64	0.97
Point 3	0.16	0.54	1.72	1.0

323

324

325 **3.2. Influence of tested mitigation strategies**

326

327 Figure 5a compares simulated daily air temperature fluctuation for all the modelled scenarios realized
328 to assess the effect of an extended application of the green systems all over the experimental set-up at
329 Puigverd de Lleida, i.e. real geometrical configuration (AR=0.33), coupled with different pavements
330 of the area, i.e. bare soil (_B), and artificial covers presenting low (_La), medium (_Ma), and high
331 albedo (_Ha). In particular, plotted air temperature profiles (Figure 5a) are computed as the average
332 among air temperature data extracted at the four reference points highlighted in the scheme of Figure
333 5b at 1.5 m height. This procedure allows to get a mean-profile of the inner cubicle boundary
334 conditions not being affected by specific canyons' orientation.

Greenery, applied alternatively both on the cubicles rooftop and southern wall, has very slight effect on the microclimate in terms of air temperature differences which are not even appreciable in Figure 5a with a temperature resolution of 2°C, i.e. y axis unit. On the contrary, differences are more significant varying the pavement surface albedo, especially during daytime, i.e. 7:00 am – 8:00 pm.

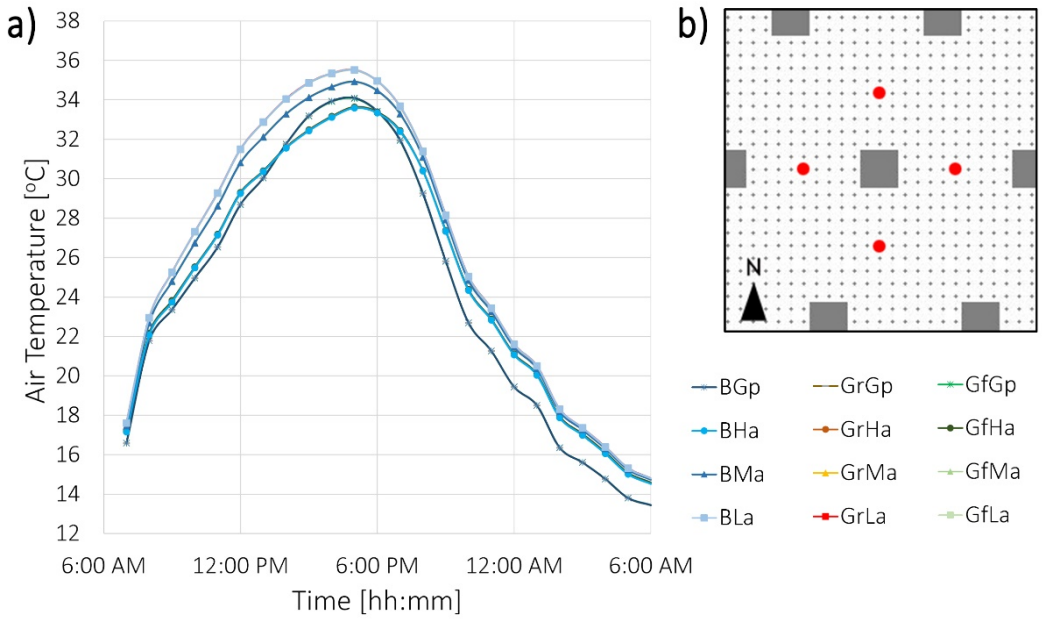

Figure 5. (a) Air temperature time-trend for all the simulated scenarios at the original configuration, i.e. AR (3/9); (b) reference points in the model where air temperature values are extracted to obtain the average profiles plotted.

It is well known that surface albedo affects the reflection of the solar radiation which can absorb less heat and stay cooler [34]. Nevertheless, the lowest temperature is obtained with the original natural bare terrain, i.e. ground of Puigverd de Lleida (_Gp), from 6:00 am until 1:00 pm. The obtained result is due to the water content of the permeable mean which allows to cool the superficial temperature (Figure 6d). As a matter of fact, evaporated water converts part of the incoming energy into latent heat flux while the artificial surfaces only release the sensible component responsible for the pavement temperature increase (Figure 6a-d). Moreover, the albedo of the natural terrain is always higher than the albedo of the low albedo (_La) scenario, varying in between 0.17 and 0.30 with a maximum soil water content of 41.8% (Figure 6d). Afterwards, the air temperature in the high albedo (_Ha) scenario is the lowest just after the hours of maximum incoming radiation, i.e. from 2:00 pm to 6:00 pm. The observed air temperature reduction is mainly imputable to the lower amount of pavement re-emitted

longwave radiation while the highest reflection does not produce a temperature increment since it preserves the energy peak in the shortwave range avoiding energy to be transformed in heat.

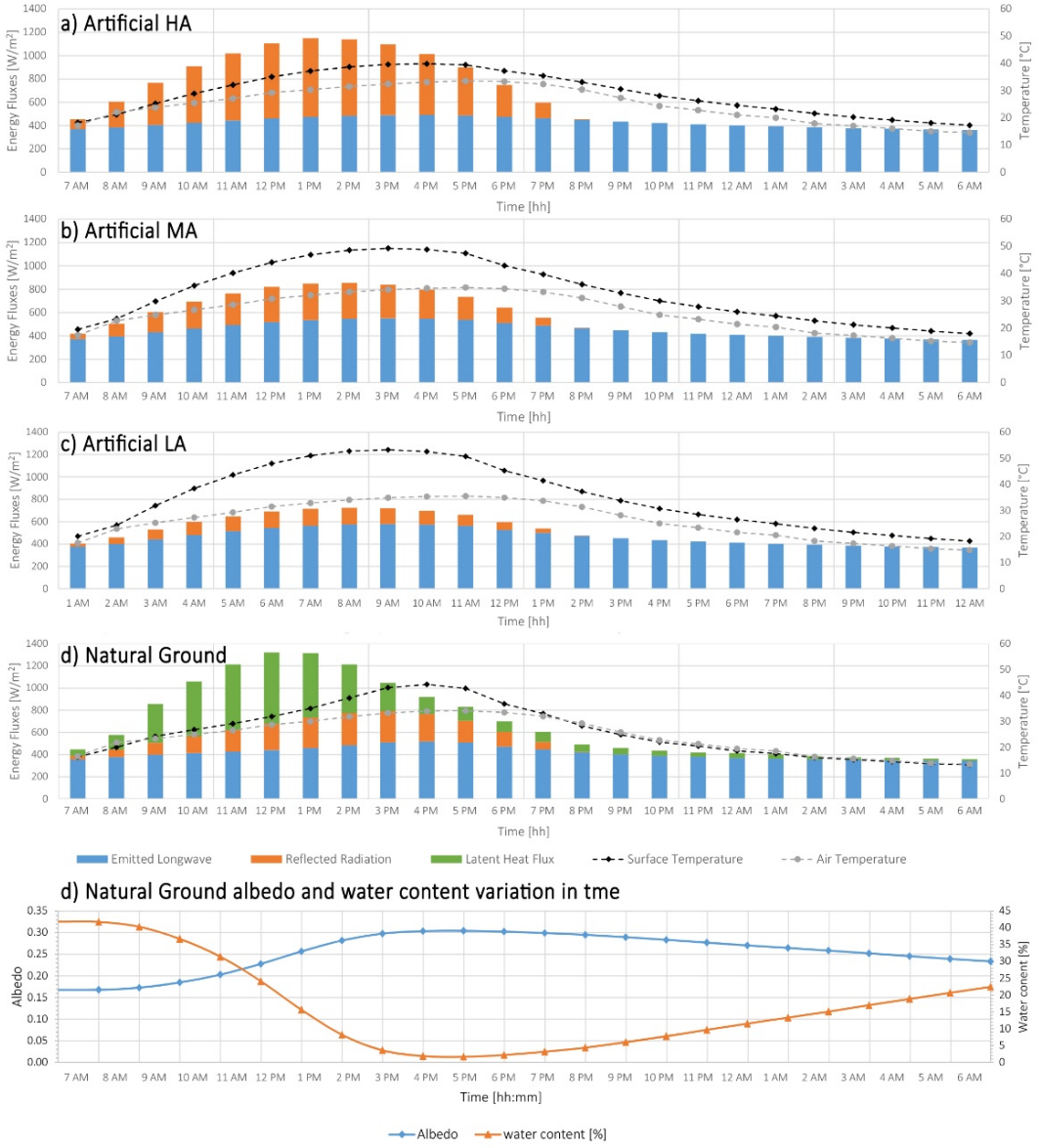

Figure 6. 24 h time trends of: (a-d) air at 1.5 m and ground superficial temperature coupled to ground outgoing heat fluxes (sensible and latent) and reflected radiation at 1.5 m for the four different typologies of modelled pavement and (d) natural ground albedo and water content.

Figure 7 shows the presented outcomes, limited to the most effective cool scenarios, in terms of air temperature distribution at 1.5 m. During the cooling down hours, i.e. 6:00 am and 12:00 am, scenarios having artificial soils, denser than the natural one, are warmer. Among them, the high albedo scenario, i.e. _Ha, has the lowest air temperature since the pavement surface remains cooler during the day. During the heating up hours, i.e. 11:00 am and 4:00 pm, artificial soils are still warmer

except for the high albedo scenario which presents the lowest air temperature values at the temperature peak time.

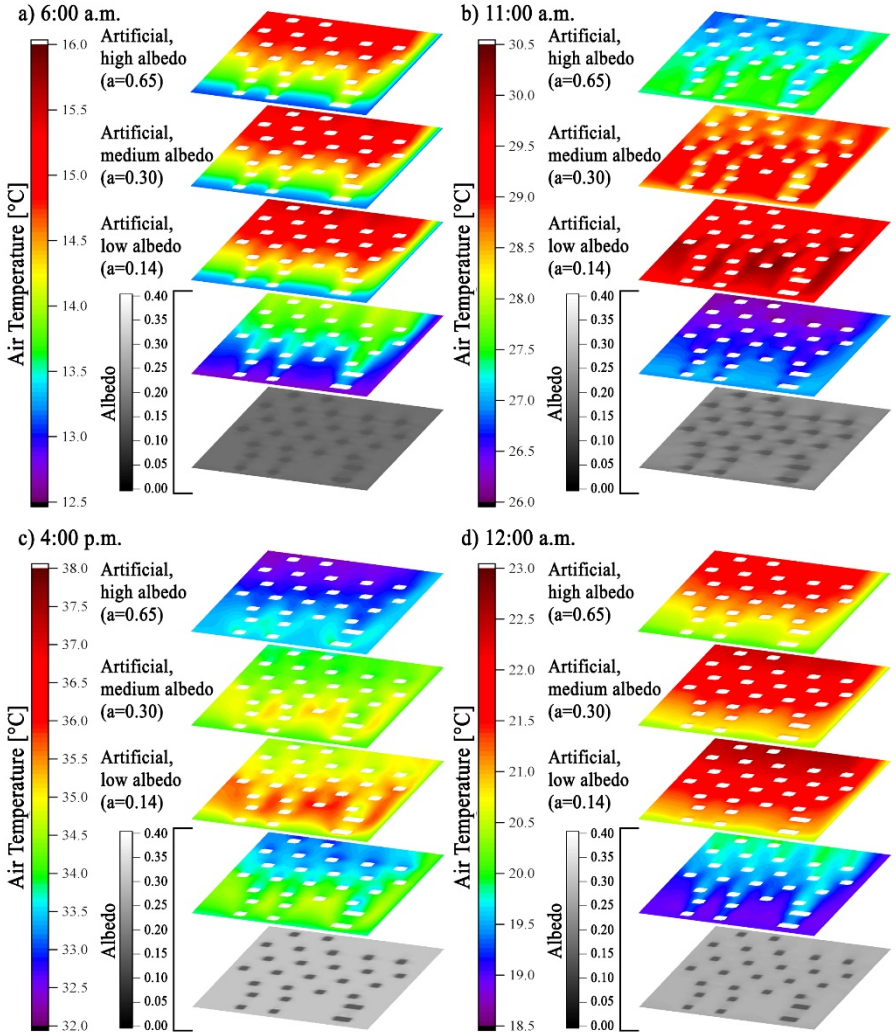

Figure 7. Air temperature spatial distribution at pedestrian level, i.e. 1.5 m, of different albedo scenarios at (a) 6 am (b) 11 am (c) 4 pm and (d) 12 am. At the bottom of each series of maps, the spatial distribution of the natural ground albedo at its surface is given.

As mentioned before, the presented results highlight that greenery has very little effect. That result may be imputable to the different extent of the green surfaces compared to the total amount of modelled built elements and to the pavement surface at disposal for the cool pavement implementation (Table 5). Therefore, the cooling effect of the greenery [35] [36] [37] and its potential in buildings energy savings [24][38] which is well known and demonstrated in the literature, it seems to be slightly punished in this case.

387
388
389
390

Table 5. Representing surfaces of the case study

m^2 of modelled pavement	4939 m^2	% of the total pavement
m^2 of modelled green roofs	261 m^2	5.3
m^2 of modelled green facades	267 m^2	5.4

391

392 Nevertheless, the effect of the green facades and green roofs is better shown in its spatial distribution
393 through the maps of Figure 8. Such maps are calculated overall the modelled area at 1.5 and 3.5 m
394 from the ground at 6:00 am, 11:00 am, 4:00 pm, and 12:00 am. Green facades have a slight cool
395 potential in their proximity especially during the day-time, i.e. at 11 am and 4 pm, losing intensity
396 increasing the albedo of the pavement (Figure 8a). In particular, the application of green facades leads
397 to slight higher air temperature in the case of high albedo scenario. Green roofs are even less effective
398 especially at pedestrian level, i.e. 1.5 m. The better results are observed at night, i.e. 6 am, with a
399 maximum temperature decrease of 0.1°C just above the rooftop (3.5 m from the ground). The effect in
400 terms of air temperature reduction decreases with pavement of higher albedo as already observed for
401 green facades.
402

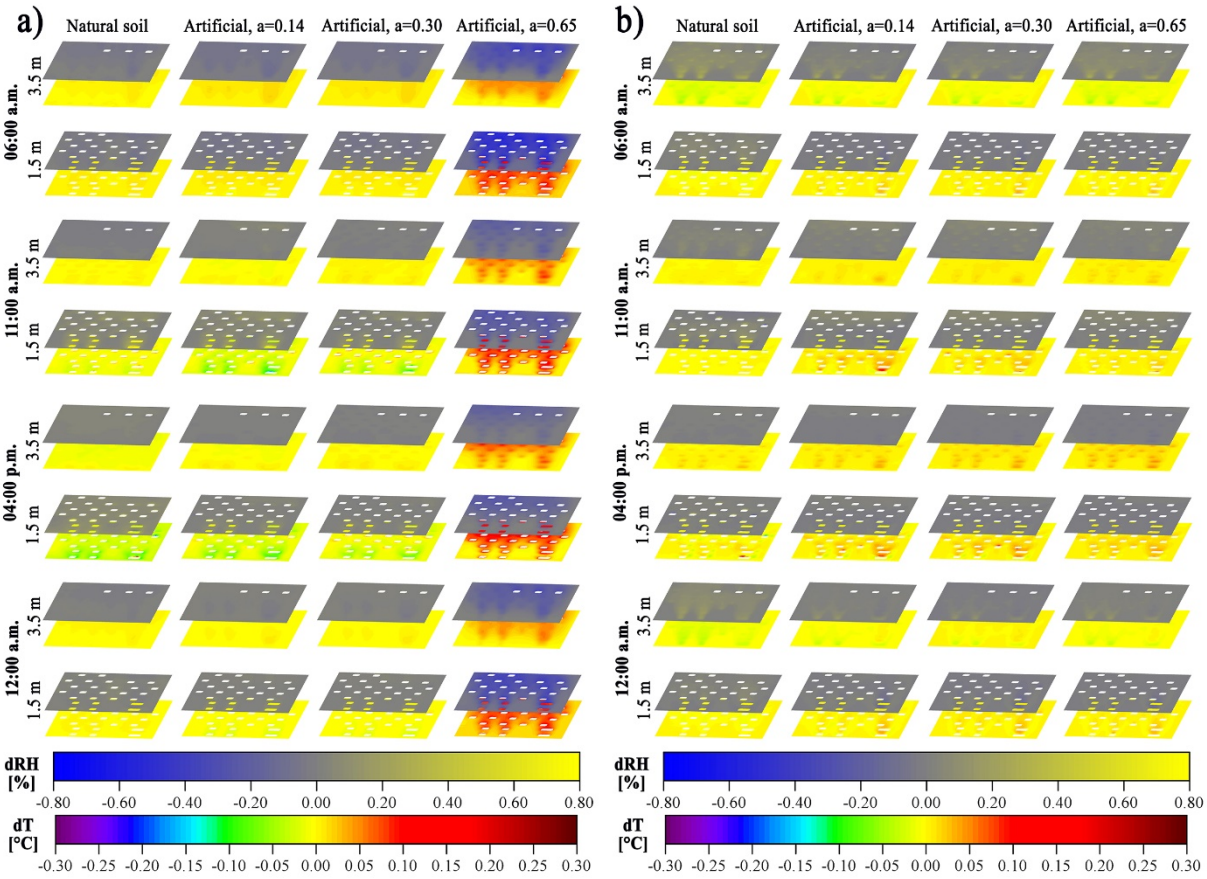

Figure 8. Spatial distribution at both 1.5 and 3.5 m above the ground of air temperature and relative humidity differences between the Basic scenario and the (a) Green Facades and (b) Green Roofs ones.

Relative humidity varies accordingly to the air temperature so no significant effects due to evapotranspiration phenomenon could be recognized at this scale. Nevertheless, it is important to remember that on a huge scale, the evapotranspiration phenomenon makes clears effects [39].

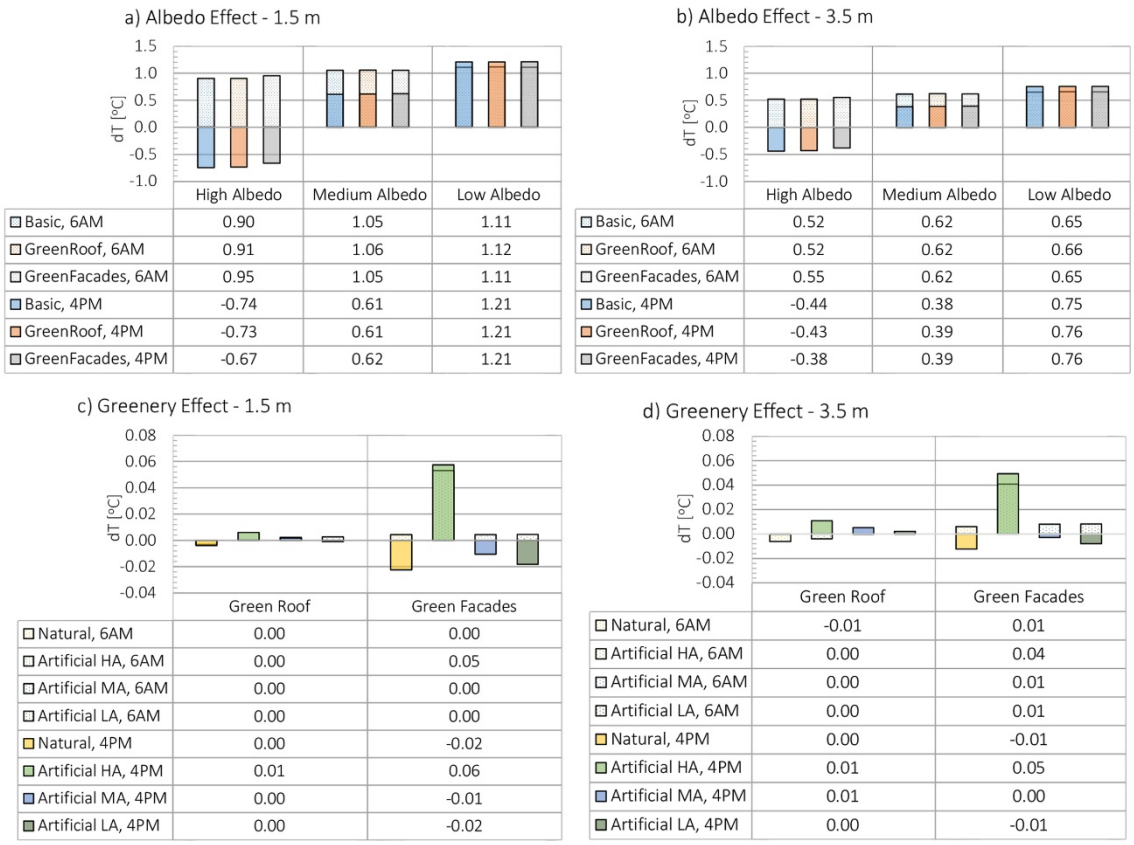

Figure 9. Temperature variation due to pavement modification (a, b) and greenery implementation (c, d) at 6 am and 4 pm.

Figure 9 summarizes the effect of both cool pavements and greenery. The presented temperature differences are calculated taking into account the corresponding scenarios with natural terrain as references to get the cool effect in Figure 9a,b. On the other hand, the reference scenarios considered to evaluate the greenery effect are the corresponding ones with no green elements. The plotted values are the average of the temperature differences observed at the four selected points (Figure 5b) during the hours of minimum and maximum air temperature peaks, i.e. 6 am and 4 pm respectively. Results are given both at pedestrian height, i.e. 1.5 m (Figure 9a,c), and above the roof level, i.e. 3.5 m (Figure 9b,d). The maximum cooling effect due to the implementation of cool pavements is equal to -0.74ºC, and is obtained close to the surface, i.e. 1.5 m, and in absence of greenery. On the other hand, green facades seem more effective with respect to green roofs especially at pedestrian height, i.e. 1.5 m, leading to a maximum reduction of -0.02ºC in the basic scenario, i.e. no cool pavement applied. In addition, Santamouris [6] said in his study that concerning the roofs (cool and green roofs), both technologies can lower the surface temperatures of roofs and thus decrease the corresponding sensible heat flux to the atmosphere. In that case, when we combine green roof with high albedo pavement the temperature increases. It can be confirmed that the variation in surface albedo of the pavements strongly influences the impact of the results.

3.3. Influence of distance between modelled buildings prototypes

The original experimental setup presents an aspect ratio of 0.33, i.e. AR 3/9, with a distance between each cubicles of 9 m. Therefore, the cubicles mutual-distance is reduced to understand the influence of both cool pavement and greenery varying the modelled area geometrical configuration. The studied cubicles-mutual-distances are 9 m, 5 m, and 3 m corresponding at an aspect ratio of 0.33, 0.6, and 1, respectively. Figure 10 summarizes the effects of the geometrical configuration in terms of air temperature variation at pedestrian height, i.e. 1.5 m.

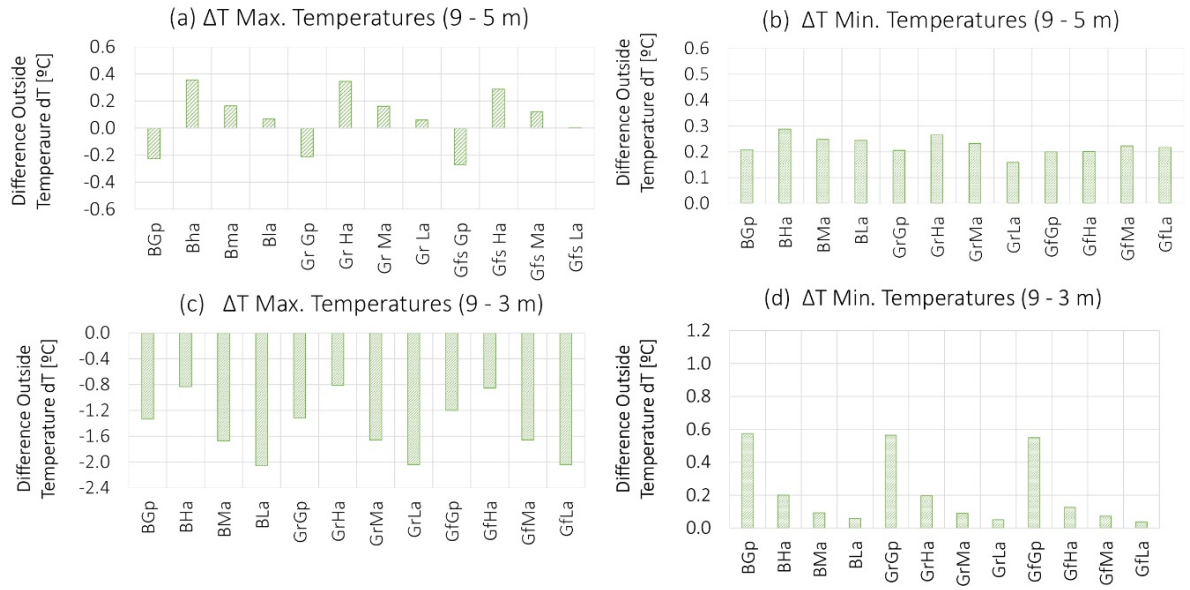

Figure 10. Differences between (a) reached maximum temperature in AR 3/9 and AR 3/5 scenarios; (b) reached minimum temperature in AR 3/9 and AR 3/5 scenarios; (c) reached maximum temperature in AR 3/9 and AR 3/3 scenarios; (d) reached minimum temperature in AR 3/9 and AR 3/5 scenarios.

By reducing the distance from 9 m to 5 m (Figure 10 a,b), a general increase of the minimum temperatures is observed up to +0.3ºC reached in the basic, i.e. no greenery, high albedo pavement scenario, i.e. BHa. Such differences are smoother in presence of greenery which buffers the increasing effect due to the more packed configuration. The effect on maximum temperatures is not consistent through all the scenarios. A reduction of the temperature maximum peak is observed only among bare natural ground models, i.e. _Gp, down to -0.3ºC in presence of green facades, i.e. GfGp scenario. On the contrary, an increase of the maximum temperature peak, proportional to the albedo level, is highlighted in all the artificial pavement modelled configurations meaning that the mitigation

potential associated to the high reflectance of the ground is reasonably less effective is more packed urban environment. The outlined results are explained considering the incoming shortwave and longwave radiative fluxes and observing the daily air and superficial temperature fluctuation (Figure 11). Plots of Figure 11a-b are the daily profile of the averaged air and superficial temperature respectively for all the simulated scenarios with an aspect ratio of 0.6, i.e. AR=3/5. Similarly, the shadow effect is presented averaging the shadow flag, i.e. integer value between 0 (no shadow) and 1 (shadow), extracted at ground level for each one of the four selected points across the 24 hours. Figure 11c shows the difference between the above presented superficial temperature data and the values of superficial temperatures and shadow flags derived for the corresponding scenarios with an aspect ratio of 0.33, i.e. AR(3/9). Highest air temperature is observed in low albedo scenarios while lowest air temperature profiles refer to natural ground models as previously observed for the reference configuration, i.e. AR(3/9). As a matter of fact, superficial temperature, and consequently longwave radiation flux from the ground, are lower in all the scenarios with natural terrain, i.e. _Gp. Such effect is due to the concentration of the evapotranspiration effect during the not shaded hours, just before the air temperature maximum peak (Figure 11b), when the latent component of the energy budget rises as a consequence of the cubicles mutual-distance reduction. Concerning scenarios with artificial pavements, the higher is the albedo, the lower is the superficial temperature consistently with analysed outcomes of the original configuration' simulations, i.e. AR(3/9). Nevertheless, superficial temperature of the high albedo pavement is slight higher in the more packed scenario, i.e. in the AR(3/5), with respect to the reference one when the surface is not shaded, as observed in Figure 11c. This is probably due to an increase radiative trapping phenomenon among the pavement and the vertical surfaces of the model, i.e. cubicles walls. This superficial temperature increase causes a general air temperature rise at 1.5 m from the ground, interacting with the thermal balance of the human body.

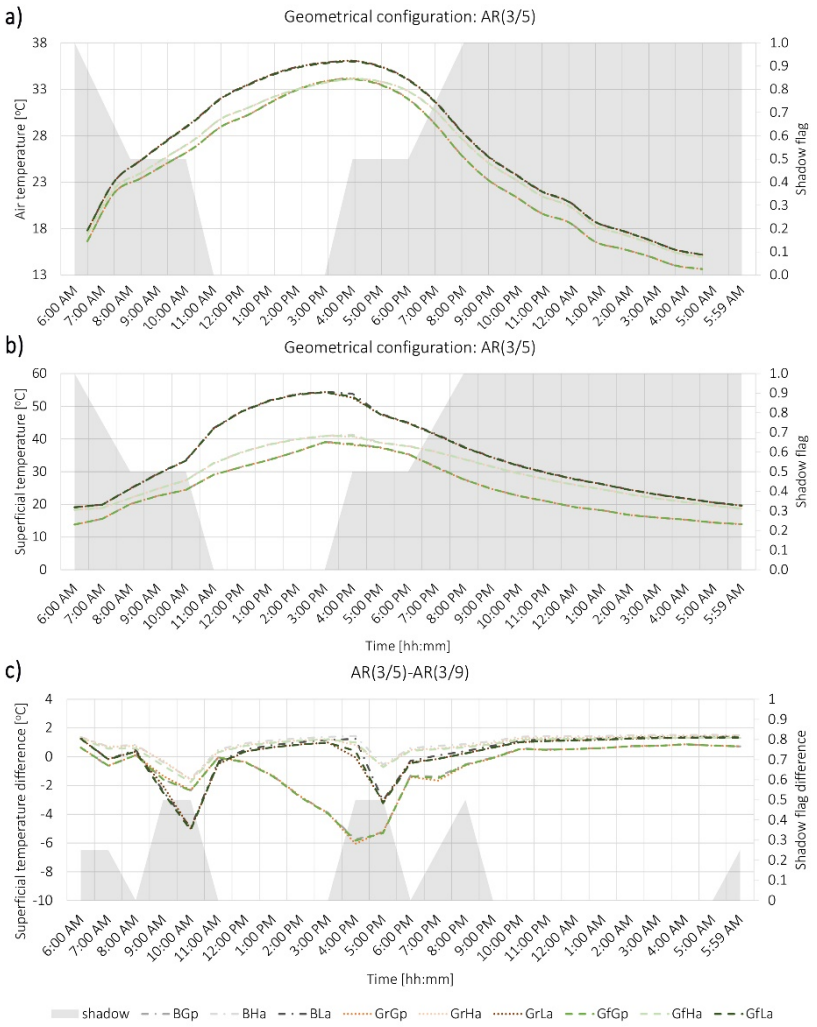

Figure 11. 24 hours trend of (a) air and (b) superficial temperature and shadow flag for all the scenarios with aspect ratio of 0.6, i.e. AR(3/5); (c) daily superficial temperature and shadow flag difference between each scenario AR(3/5) and the correspondent one with the original geometrical configuration, i.e. AR(3/9).

By reducing the distances among cubicles down to 3 m, a general buffer of the daily temperature fluctuations is highlighted for all the modelled scenarios (Figure 10c,d). Therefore, the air temperature minimum peak increases up to +0.6°C observed in BGp scenario, i.e. natural terrain and no greenery. On the contrary, the daily maximum peak decreases in all the modelled scenarios down to a maximum reduction of -2.1°C observed with low albedo pavements, i.e. BLa, GrLa, and GfLa scenarios. The application of the green systems seems not to influence the outlined changes due to different geometrical configuration of the modelled area exception made for slight general reductions of temperatures, both maximum and minimum peaks, observed with the presence of green facades. Even if the model dimensions are generally reduced, the amount of greenery is still not comparable to the pavement extent (Table 6).

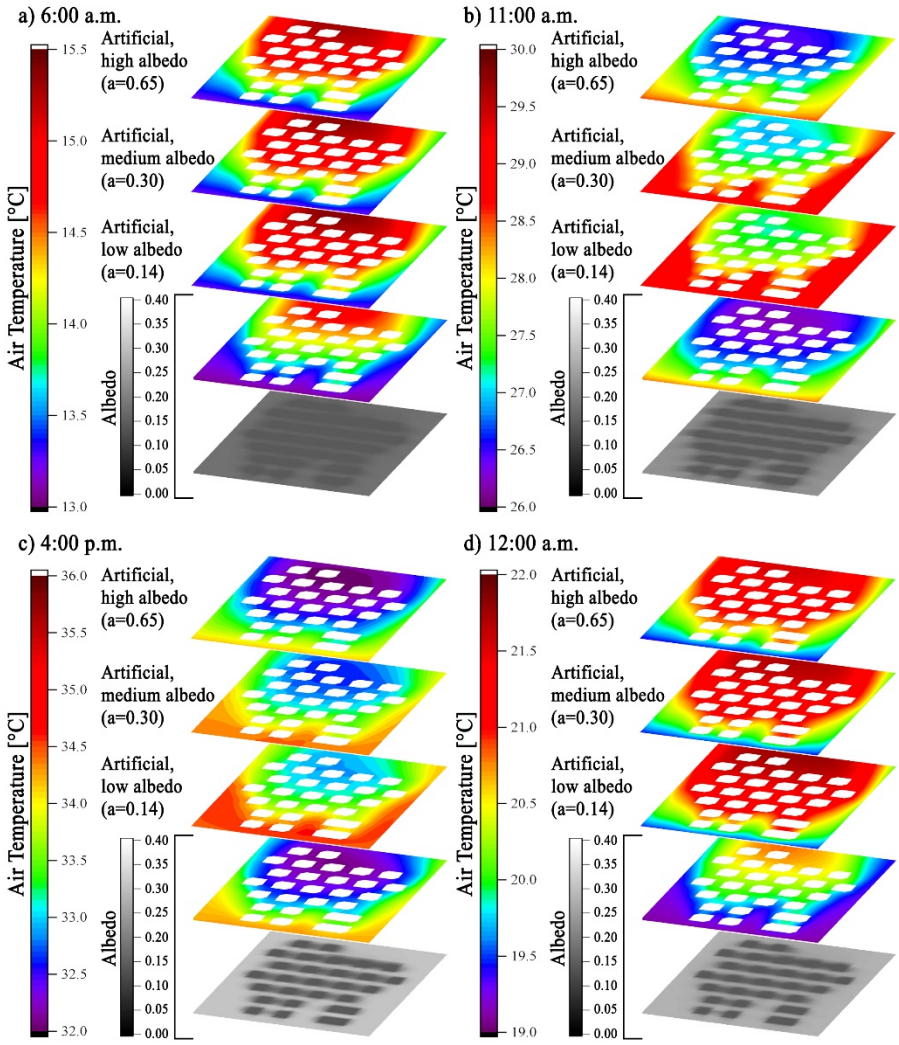

Figure 12. Air temperature spatial distribution within the area at pedestrian level, i.e. 1.5 m, of different albedo scenarios at (a) 6 am, (b) 11 am, (c) 4 pm, and (d) 12 am. At the bottom of each series of maps, the spatial distribution of the natural ground albedo at its surface is given. Aspect ratio of 1.

Table 6. Representing surfaces of the case study

	AR (3/9)	AR (3/5)	AR (3/3)	AR (3/9)	AR (3/5)	AR (3/3)
m^2 of pavement studied	4939 m^2	2512 m^2	1525 m^2	% of the total pavement		
m^2 of green roofs studied	261 m^2	261 m^2	261 m^2	5.3	10.4	17.1
m^2 of green facades studied	267 m^2	267 m^2	267 m^2	5.4	10.6	17.5

Finally, the spatial distribution of the air temperature is analysed across all the simulated scenarios characterized by the highest density, i.e. aspect ratio of 1, through the maps presented in Figure 12 and Figure 13. The slight air temperature increase observed during day-time, i.e. at 11 am and 4 pm,

in the green facades scenarios could be imputed to a leaf temperature rise which can alter air temperature in such dense configuration. Nevertheless, the adopted version of the simulation engine does not allow to check this information and no data could prove the presented hypothesis.

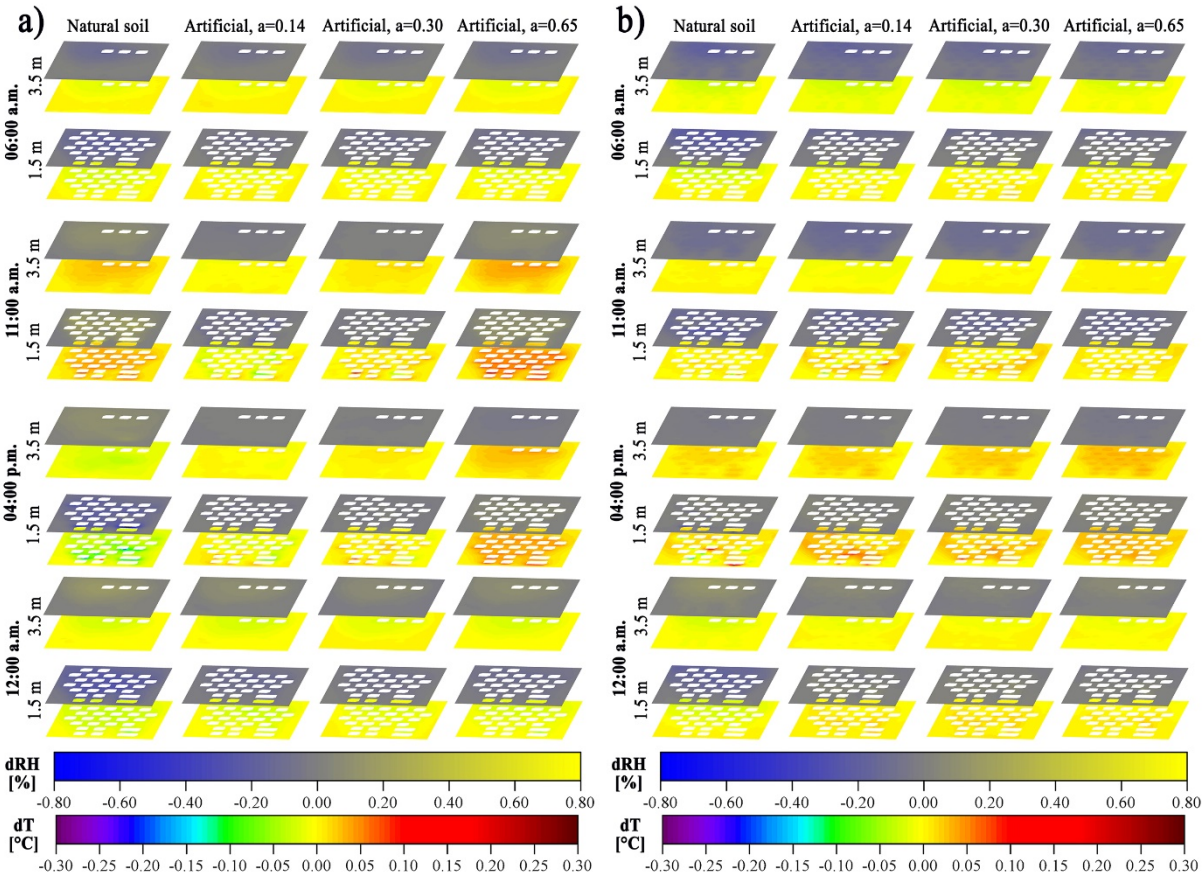

Figure 13. Spatial distribution at both 1.5 m and 3.5 m above the ground of air temperature and relative humidity differences between the Basic scenario and the (a) Green Facades and (b) Green Roofs ones.

4. Conclusions

Local scale climate change mitigation has become an urgent need for improving indoor and outdoor wellbeing, and key mitigation strategies, e.g. cool pavements, greenery and water bodies, demonstrated their effectiveness in both real and modelled urban environments. This study wants to bridge the gap between analysis in real fields, typically affected by the specific urban configuration also characterized by further uncontrollable anthropogenic actions, and lab scale experiments and numerical models. This is carried out by means of a dedicated investigation of an experimental field in Puigverd de Lleida (Spain) where more than 20 house-like cubicles are continuously monitored to test different passive and active buildings energy saving techniques. The simplified built environment

area is modelled and simulated after calibration and validation by means of an internationally acknowledged CFD modelling tool. The effect of the considered mitigation strategies on the outdoor modelled environment, is studied in terms of air temperature and radiation budget, with varying the geometrical configuration of the model with the final aim to assess how their contribution could be sensitive to varying cubicles mutual distance and model aspect ratio (i.e. cubicle height on cubicle mutual distance ratio) representing the experimental field compactness.

The analysis demonstrates that in the analysed experimental field, high albedo pavements lead to a general significant passive air cooling during the whole day, reducing air temperature especially in presence of direct solar radiation and therefore during the hottest hours of the day, as perceived at pedestrian level. On the other side, the interpretation of the outputs related to greenery implementation is relatively more controversial and does not report the expected mitigation effect of vegetation in terms of air temperature passive cooling, widely proved by experimental studies. Generally higher temperature during day-time and lower temperature at night are detected for both the simulated greenery systems (i.e. green roofs and facades). The main reason could be imputed to the temperature rise of the leafs during the sunny hours due to their low albedo, as it has been measured by albedometer on site. Therefore, foliage albedo should be better selected and enhanced in order to achieve the required passive cooling effect to be perceived by pedestrians, if the greenery design is meant to behave as a local overheating mitigation tool.

Results concerning the analysis of environmental data related to the geometrical configuration of the modelled area show that both tested system (green roof and green facades) are more effective in denser contexts (higher aspect ratio) and in low albedo contexts. In particular, when the aspect ratio is equal to 1, albedo is the key variable to decrease air temperature maximum peak. At the same time, this study shows that higher density corresponded to higher minimum air temperature conditions meaning that experimental field compactness reduces incoming solar radiation at pedestrian level during the day and traps longwave re-emitted radiation from built surfaces at night. Concerning the effectiveness of green systems in more compact contexts, the case study environment is characterized by a real maximum aspect ratio equal to 1, while realistic compact and very dense urban systems are typically characterized by much higher aspect ratio values and taller buildings, where their roofs are relatively much far away from pedestrians to be perceived at ground level. In this case, green roofs position may be considered as close enough to be perceived by pedestrians in terms of their mitigation potential. For this reason, the achieved results may be considered as acceptable of the specific case, even if in contrast with the main findings of literature about much denser urban systems.

Therefore, this study demonstrates how specific real field studies, even if absolutely representative of the site specific conditions, may not be used for quantitatively extend microclimate mitigation results of single intervention, while the presented experimental field due to its simplified geometry allows a better control of single environmental variable effect on local microclimate. Moreover, building prototypes dimensions guarantee higher accuracy in data collection with respect to downscaled lab models to drive urban design strategies. Therefore, the modelled alternative scenarios and obtained simulation results could be validated once more by implementing the proposed strategies in the experimental field. In this view, a more consistent and massive effort should be played by local authorities and public government institution to support wide assessments in all the urban areas affected by UHI phenomenon, as responsible for the exacerbation of increasing health risks in dense urban contexts which are predicted to become even more severe in the next decades [29].

As a limitation of this analysis, the authors specify that all these results may be considered as representative of the Mediterranean continental climate, and they are not directly applicable to all climates. For this reason, as a next step of the study, a consistency analysis between the case study experimental field and a more realistic implementation will be carried out with considering a variety of urban morphologies, including the typical aspect ratios of urban canyons in both historical centres and modern suburbs in Europe, in order to qualitatively elaborate data-driven urban design guidelines reporting the best solutions applicable in different contests and the possible achievable benefits. In this view, the present study may be considered as a further step forward the scientific and environmental challenge to improve wellbeing in the built environment affected by anthropogenic actions. Additionally, going toward a more detailed analysis of inter-urban microclimate is also necessary to optimize renewable energy production at district scale which is a valuable strategy to reduce carbon-foot-print of the building stock in the main frame of sustainable development.

Acknowledgements

The work is partially funded by the Spanish government ENE2015-64117-C5-1-R (MINECO/FEDER) and ULLE10-4E-1305 and SOS CITTA' (Fondazione Cassa di Risparmio di Perugia, (2018.0499.026). The authors would like to thank the Catalan Government for the quality accreditation given to their research group (2017 SGR 1537) and the city hall of Puigverd de Lleida. GREiA is a certified agent TECNIO in the category of technology developers from the Government of Catalonia. Marta Chàfer would like to thank the program Spanish Universities for EU Projects from Campus Iberus for the mobility scholarship. Ilaria Pigliautile would like to acknowledge the PhD Course of Energy and Sustainable development at University of Perugia and H2CU centre for

supporting her international activities and scientific collaborations during the course of her PhD. The authors from University of Perugia also thank UNESCO Chair on "Water Resources Management and Culture", and the Honors Center of Italian Universities (H2CU) for supporting their studies on wellbeing.

References

[1] U. Berardi, The outdoor microclimate benefits and energy saving resulting from green roofs retrofits, Energy Build. 121 (2016) 217–229. doi:10.1016/j.enbuild.2016.03.021.

[2] H. Akbari, H. Taha, The impact of trees and white surfaces on residential heating and cooling energy use in four Canadian cities, Energy. 17 (1992) 141–149. doi:10.1016/0360-5442(92)90063-6.

[3] D.J. Sailor, A holistic view of the effects of urban heat island mitigation, in: S. Lehmann (Ed.), Low Carbon Cities Transform. Urban Syst., 2014: pp. 270–281.

[4] P. Bosselmann, E. Arens, K. Dunker, R. Wright, Urban Form and Climate: Case Study, Toronto, 1995. doi:10.1080/01944369508975635.

[5] M.A. Hart, D.J. Sailor, Quantifying the influence of land-use and surface characteristics on spatial variability in the urban heat island, Theor. Appl. Climatol. 95 (2009) 397–406. doi:10.1007/s00704-008-0017-5.

[6] M. Santamouris, L. Ding, F. Fiorito, P. Oldfield, P. Osmond, R. Paolini, D. Prasad, A. Synnefa, Passive and active cooling for the outdoor built environment – Analysis and assessment of the cooling potential of mitigation technologies using performance data from 220 large scale projects, Sol. Energy. 154 (2017) 14–33. doi:10.1016/j.solener.2016.12.006.

[7] R. Paolini, A.G. Mainini, T. Poli, L. Vercesi, Assessment of thermal stress in a street canyon in pedestrian area with or without canopy shading, Energy Procedia. 48 (2014) 1570–1575. doi:10.1016/j.egypro.2014.02.177.

[8] M. Santamouris, S. Haddad, M. Saliari, K. Vasilakopoulou, A. Synnefa, R. Paolini, G. Ulpiani, S. Garshasbi, F. Fiorito, On the energy impact of urban heat island in Sydney: Climate and energy potential of mitigation technologies, Energy Build. 166 (2018) 154–164. doi:10.1016/J.ENBUILD.2018.02.007.

[9] R. Paolini, F. Antretter, F. Cotana, A.L. Pisello, M. MeshkinKiya, A. Zani, T. Poli, V.L. Castaldo, The hygrothermal performance of residential buildings at urban and rural sites: Sensible and latent energy loads and indoor environmental conditions, Energy Build. 152 (2016) 792–803. doi:10.1016/j.enbuild.2016.11.018.

[10] F. Rosso, A.L. Pisello, F. Cotana, M. Ferrero, On the thermal and visual pedestrians'

633 perception about cool natural stones for urban paving: A field survey in summer conditions,
634 Build. Environ. 107 (2016) 198–214. doi:10.1016/j.buildenv.2016.07.028.
635 [11] A.L. Pisello, C. Piselli, F. Cotana, Influence of human behavior on cool roof effect for summer
636 cooling, Build. Environ. 88 (2015) 116–128. doi:10.1016/j.buildenv.2014.09.025.
637 [12] C. Efthymiou, M. Santamouris, D. Kolokotsa, A. Koras, Development and testing of
638 photovoltaic pavement for heat island mitigation, Sol. Energy. 130 (2016) 148–160.
639 doi:10.1016/j.solener.2016.01.054.
640 [13] F. Laureti, L. Martinelli, A. Battisti, Assessment and Mitigation Strategies to Counteract
641 Overheating in Urban Historical Areas in Rome, Climate. 6 (2018) 18.
642 doi:10.3390/cli6010018.
643 [14] F. Salata, I. Golasi, A.D.L. Vollaro, R.D.L. Vollaro, How high albedo and traditional
644 buildings' materials and vegetation affect the quality of urban microclimate. A case study,
645 Energy Build. 99 (2015) 32–49. doi:10.1016/j.enbuild.2015.04.010.
646 [15] F. Salata, I. Golasi, R. de Lieto Vollaro, A. de Lieto Vollaro, Outdoor thermal comfort in the
647 Mediterranean area. A transversal study in Rome, Italy, Build. Environ. 96 (2016) 46–61.
648 doi:10.1016/j.buildenv.2015.11.023.
649 [16] F. Rosso, I. Golasi, V.L. Castaldo, C. Piselli, A.L. Pisello, F. Salata, M. Ferrero, F. Cotana, A.
650 de Lieto Vollaro, On the impact of innovative materials on outdoor thermal comfort of
651 pedestrians in historical urban canyons, Renew. Energy. 118 (2018).
652 doi:10.1016/j.renene.2017.11.074.
653 [17] W. Nyuk Hien, Urban heat island research: Challenges and potential, Front. Archit. Res. 5
654 (2016) 276–278. doi:10.1016/j.foar.2016.04.001.
655 [18] D. Kannamma, A.M. Sundaram, Implications of building material choice on outdoor
656 microclimate for sustainable built environment, Key Eng. Mater. 650 (2015) 82–90.
657 doi:10.4028/www.scientific.net/KEM.650.82.
658 [19] C.L. Tan, N.H. Wong, S.K. Jusuf, Effects of vertical greenery on mean radiant temperature in
659 the tropical urban environment, Landsc. Urban Plan. 127 (2014) 52–64.
660 doi:10.1016/j.landurbplan.2014.04.005.
661 [20] A. Gros, E. Bozonnet, C. Inard, Cool materials impact at district scale - Coupling building
662 energy and microclimate models, Sustain. Cities Soc. 13 (2014) 254–266.
663 doi:10.1016/j.scs.2014.02.002.
664 [21] E. Andreou, The effect of urban layout, street geometry and orientation on shading conditions
665 in urban canyons in the Mediterranean, Renew. Energy. 63 (2014) 587–596.
666 doi:10.1016/j.renene.2013.09.051 Technical note.
667 [22] E. Ng, L. Chen, Y. Wang, C. Yuan, A study on the cooling effects of greening in a high-
668 density city: An experience from Hong Kong, Build. Environ. 47 (2012) 256–271.

669 doi:10.1016/j.buildenv.2011.07.014.
670 [23] A. de Gracia, L. Navarro, J. Coma, S. Serrano, J. Romaní, G. Pérez, L.F. Cabeza,
671 Experimental set-up for testing active and passive systems for energy savings in buildings –
672 Lessons learnt, Renew. Sustain. Energy Rev. 82 (2018) 1014–1026.
673 doi:10.1016/j.rser.2017.09.109.
674 [24] J. Coma, G. Pérez, A. de Gracia, S. Burés, M. Urrestarazu, L.F. Cabeza, Vertical greenery
675 systems for energy savings in buildings: A comparative study between green walls and green
676 facades, Build. Environ. 111 (2017) 228–237. doi:10.1016/j.buildenv.2016.11.014.
677 [25] G. Pérez, J. Coma, S. Sol, L.F. Cabeza, Green facade for energy savings in buildings: The
678 influence of leaf area index and facade orientation on the shadow effect, Appl. Energy. 187
679 (2017) 424–437. doi:10.1016/j.apenergy.2016.11.055.
680 [26] M.C. Peel, B.L. Finlayson, T.A. McMahon, Updated world map of the Köppen-Geiger climate
681 classification, Hydrol. Earth Syst. Sci. 11 (2007) 1633–1644. doi:10.5194/hess-11-1633-2007.
682 [27] S. Huttner, M. Bruse, Numerical modeling of the urban climate - a preview on ENVI-MET
683 4.0, Seventh Int. Conf. Urban Clim. (2009) 1–4.
684 [28] F. By, NUMERICAL METHODS USED IN ATMOSPHERIC MODELS, I (n.d.).
685 [29] no. 4 (2000): 49-56. Crawley, Drury B., Linda K. Lawrie, Curtis O. Pedersen, and Frederick
686 C. Winkelmann. “Energy plus: energy simulation program.” ASHRAE journal 42, No Title,
687 (n.d.).
688 [30] C.J. Willmott, Some Comments on the Evaluation of Model Performance, Am. Meteorol. Soc.
689 63 (1982) 1309–1313. doi:10.1175/1520-0477(1982)063<1309:SCOTEO>2.0.CO;2.
690 [31] C. Bartesaghi Koc, P. Osmond, A. Peters, Evaluating the cooling effects of green
691 infrastructure: A systematic review of methods, indicators and data sources, Sol. Energy. 166
692 (2018) 486–508. doi:10.1016/j.solener.2018.03.008.
693 [32] A. Zhang, R. Bokel, A. van den Dobbelsteen, Y. Sun, Q. Huang, Q. Zhang, An integrated
694 school and schoolyard design method for summer thermal comfort and energy efficiency in
695 Northern China, Build. Environ. 124 (2017) 369–387. doi:10.1016/j.buildenv.2017.08.024.
696 [33] F. Salata, I. Golasi, R. de Lieto Vollaro, A. de Lieto Vollaro, Urban microclimate and outdoor
697 thermal comfort. A proper procedure to fit ENVI-met simulation outputs to experimental data,
698 Sustain. Cities Soc. 26 (2016) 318–343. doi:10.1016/j.scs.2016.07.005.
699 [34] A.L. Pisello, State of the art on the development of cool coatings for buildings and cities, Sol.
700 Energy. 144 (2017) 660–680. doi:10.1016/j.solener.2017.01.068.
701 [35] M. Huang, P. Cui, X. He, Study of the Cooling Effects of Urban Green Space in Harbin in
702 Terms of Reducing the Heat Island Effect, (2018) 1–17. doi:10.3390/su10041101.
703 [36] H.M.P.I.K. Herath, R.U. Halwatura, G.Y. Jayasinghe, Evaluation of green infrastructure
704 effects on tropical Sri Lankan urban context as an urban heat island adaptation strategy, Urban

For. Urban Green. 29 (2018) 212–222. doi:10.1016/j.ufug.2017.11.013.

[37] T. Susca, S.R. Gaffin, G.R. Dell'Osso, Positive effects of vegetation: Urban heat island and green roofs, Environ. Pollut. 159 (2011) 2119–2126. doi:10.1016/j.envpol.2011.03.007.

[38] G. Vox, I. Blanco, E. Schettini, Green façades to control wall surface temperature in buildings, Build. Environ. 129 (2018) 154–166. doi:10.1016/j.buildenv.2017.12.002.

[39] G. yu QIU, H. yong LI, Q. tao ZHANG, W. CHEN, X. jian LIANG, X. ze LI, Effects of Evapotranspiration on Mitigation of Urban Temperature by Vegetation and Urban Agriculture, J. Integr. Agric. 12 (2013) 1307–1315. doi:10.1016/S2095-3119(13)60543-2.